Engineering with Computers (2019) 35:857–874
https://doi.org/10.1007/s00366-018-0636-0

ORIGINAL ARTICLE

A three-stage damage detection method for large-scale space structures using forward substructuring approach and enhanced bat optimization algorithm

Ramin Ghiasi[1] · Hamed Fathnejat[2] · Peyman Torkzadeh[1]

Received: 27 April 2017 / Accepted: 16 August 2018 / Published online: 20 August 2018
© Springer-Verlag London Ltd., part of Springer Nature 2018

Abstract
In this study, an efficient three-stage method is proposed for damage detection of large-scale space structures by employing forward substructuring approach, modal strain energy and enhanced bat algorithm (EBA) optimization. EBA is a modified version of BA that is proposed in this paper and used a passive congregation operator to improve the performance of standard BA. In the first stage, the global structure is divided into manageable substructures. The stiffness matrices of independent substructures are obtained based on Kron's substructuring method. Then a modal strain energy-based index is employed to precisely locate the eventual damages of the structure. In the third stage, damage severities are estimated via EBA using the second-stage results. To demonstrate the ability of the proposed method for detection of multiple structural damages, large-scale space structures with different types of damage scenarios are considered. The results show that the proposed method can detect the exact locations and severity of damages highly accurate in space structures.

Keywords Damage detection · Space structure · Substructuring method · Modal strain energy · Enhanced bat optimization algorithm

1 Introduction

Space structure is one of the large-scale structures with a great number of elements and degrees of freedom. Local damages in a space structure reduce its stiffness and thus lead to modification of the dynamic properties [1]. Structural damage detection is widely performed by comparing the static or dynamic responses of the intact structure with those of the damaged structure. For a large-scale structure, local damages usually induce slight changes to the global modal data, which makes the local damages difficult to be detected.

Structural health monitoring mainly aims at continuously tracking and evaluating the symptoms of deterioration or damage that may affect the operation, serviceability, or safety reliability of the structure [2]. The vibration-based damage identification methods are popularly used among the researchers for the nondestructive damage identification of large-scale structures. The basis of the vibration-based damage identification is that the damage-induced changes in the physical properties (mass, damping, and stiffness) will cause detectable changes in modal properties (natural frequencies, modal damping, and mode shapes). Goyal and Pabla [3] and Fan and Qiao [4] presented an extensive review of the vibration-based damage detection methods. Damage detection is usually performed by comparing the responses of the undamaged structure with those of the damaged structure. The frequencies, mode shapes, flexibility matrices, mode shape curvatures and vibration responses were frequently used for damage detection [5, 6]. Furthermore, recently some new damage detection methods and indicators were proposed by researchers such as operating deflection shape (ODS) that derived from experimental frequency response function (FRF) data [7], energy balance equation [8], generalized flexibility-based model updating approach [9], damage locating vectors [10] and Bayesian damage identification techniques [11].

✉ Ramin Ghiasi
rghiasi.s@gmail.com

1 Department of Civil Engineering, Faculty of Engineering, Shahid Bahonar University of Kerman, Kerman, Iran

2 Department of Civil Engineering, Graduate University of Advanced Technology, Kerman, Iran

One of the main difficulties associated with the use of the vibration-based damage identification methods lies in the small sensitivity of the modal parameters to the local damage. Alampalli [12] reported that the relative frequency changes of a bridge due to an artificial cut across the whole bottom flanges of both main girders were about 3–8%. The Z24 bridge in Switzerland was progressively damaged in terms of 17 scenarios [13]. The maximum frequency decrease of the first five modes was 5.9% until the most severe damage scenario. Robert and John [14] continuously monitored in-service highway bridges during the five-stage introduction of cracks in one of the main supporting girders. The maximum frequency change caused by the most severe damage was 4.2% (0.36 Hz), when the crack extended through two-thirds of the depth of the girder. For a practical structure, the damage in local area usually introduces insignificant changes of the global modal data, which are even smaller than the changes caused by the environmental and operational conditions [15]. As a result, the local damage of a structure is sometimes difficult to be detected based on the global modal data.

Several approaches have been proposed to identify the location and the severity of damages in a large-scale structure, such as that provided by Torkzadeh et al. [16]; this method was based on kinetic and modal strain energies and also Heuristic Particle Swarm Optimization (HPSO) algorithm. The results illustrated the high performance of this method but the process of estimating severity of damages was time consuming.

The substructuring method is efficient in damage detection of large-scale structures since it concerns the local area as an independent structure. As the global structure is replaced by smaller and more manageable substructures, it enables considerably easier and quicker to analyze the small substructures. In addition, substructuring methods enable the analysis and identification of local parts and thus lead to more accurate damage identification [17, 18]. Craig [17], Weng et al. [18, 19] and Xia et al. [20] proposed a forward substructuring approach for structural modeling domain. The partitioned substructures are analyzed independently to obtain their designated solutions, which are assembled to recover the solutions of the global structure by imposing constraints at the interfaces. This substructuring approach is frequently used for the calculation of eigensolutions and eigensensitivity of the global structure. During model updating or damage detection, if the local area is modified, only the modified substructure will be re-analyzed and will be assembled with other unchanged substructures to calculate the eigensolutions of the global structure. As the eigensolutions of the global structure are recovered from substructural solutions through an assembly procedure, this substructuring method is called forward substructuring approach [18].

In this study, based on previous investigations of the present authors on use of artificial intelligence (AI) methods in structural health monitoring domain [21–23], the presented methods are further extended for large-scale structures using substructure concept. Hence, an efficient three-stage method is proposed for damage detection of large-scale space structures by employing forward substructuring approach, modal strain energy and also enhanced bat algorithm (EBA) optimization.

During last years, several meta-heuristic optimization algorithms are used to reach the best solution in various domains of structural engineering such optimal design of structures [24–26], health monitoring/damage detection [27], system identification [28], etc. Among them, bat algorithm has shown great success in time-saving to search for the global optimum [25]. The bat algorithm is a population-based metaheuristic optimization algorithm which was first inspired by the behavior of the bat animals to find food. Some special characteristics such as comprehensible structure, easy implementation, the ability to both local and global, etc., make the BA such a suitable optimization tool [29].

In the first stage of the proposed method, the global structure is divided into manageable substructures. The stiffness matrices of independent substructures are obtained based on Kron's substructuring method. Then a Modal Strain Energy Based Index (MSEBI) is used to precisely locate the eventual damage of a substructure. In the third stage, the damage severities are estimated via EBA optimization using the second-stage results. For this purpose, the structural damage detection is formulated as an unconstrained optimization problem. Stiffness parameters in finite element model are also considered as the structural damage index and the damage severities are estimated based on multiple damage location assurance criterion (MDLAC) [30].

Therefore, the main contribution of this study is to introduce an effective approach based on Kron's substructuring method and EBA to implement damage detection procedure on large-scale structure. In previous studies, researchers use several methods such as modified meta-heuristic optimization algorithms that remove unchanged variable after specified number of iteration [16, 31], various two-stage damage detection methods that the decrease number of damage variable in the second-stage [31, 32] data reduction methods [33, 34], metamodeling techniques [23, 35, 36] ,and advanced methods for interpretation of the massive (big) data collected for structural health monitoring [37, 38]. However, using these methods, only specific structures can be analyzed and in most of them, the accuracy of methods will decrease if a larger structure is considered. In comparison with using proposed approach, any large-scale structure with any number of degrees of freedom DOF's can be divided into manageable substructures and then any preferred damage detection procedure can be implemented on individual substructures. Hence, proposed approach decreases some kind of "curse of dimensionality problem" in structural health monitoring (SHM) domain and it can shift the focus of the researchers from the sensing and instrumentation to the SHM data interpretation area.

In addition, another unique aspect of this study is that we enhance performance of BA by presenting a bat algorithm with passive congregation to improve the performance of standard BA. Passive congregation is an important biological force preserving bat integrity. By introducing passive congregation to BA, information can be transferred among individuals of the bat, thus making the approach more feasible for a wider range of practical applications while preserving the attractive characteristics of the basic BA.

To demonstrate the ability of the proposed method for detection of multiple structural damages, different types of damage scenarios on large-scale space structures are considered. The results show that the proposed method can detect the exact locations and the severity of damages highly accurate in these structures.

This paper is organized as follows: In Sect. 2, we describe the basic theorem of substructuring method. Damage detection indices including MDLAC and MSEBI are represented in Sect. 3. Bat optimization algorithm is described in Sect. 4. The proposed damage detection procedure is described in Sect. 5. The numerical examples are studied in Sect. 6 and conclusions are summarized in Sect. 7.

2 Basic theorem of substructuring method

For a global structure with N DOFs, its stiffness matrix and mass matrix will be in the order of $N \times N$. Application of the substructuring method firstly requires that the global structure is torn or divided into NS independent substructures [39], and each substructure has n_j DOFs ($j = 1, 2, ..., \mathrm{NS}$). This division procedure will produce NT tearing DOFs. Each tearing DOF will divide into two or more DOFs after division, i.e., a tearing DOF in the original global structure is shared by two or more substructures that are connected to it. The total number of DOFs of all substructures will be expanded to NP, which is larger than N. If the mth ($m = 1, 2, ..., \mathrm{NT}$) tearing DOF is shared by t_m substructures, we have:

$$\mathrm{NP} = N + \sum_{m=1}^{\mathrm{NT}} (t_m - 1),\ \mathrm{NP} = \sum_{j=1}^{\mathrm{NS}} n_j. \tag{1}$$

To be viewed as an independent structure, each substructure has its stiffness matrix $K^{(j)}$ and mass matrix $M^{(j)}$, $j = 1, 2, \dots, \mathrm{NS}$. The generalized eigenequation of the jth substructure can be written as:

$$K^{(j)}\{\phi_i^{(j)}\} = \lambda_i^{(j)} M^{(j)}\{\phi_i^{(j)}\}, \tag{2}$$

both the stiffness matrix $K^{(j)}$ and the mass matrix $M^{(j)}$ are in the order of $n_j \times n_j$. $\lambda_i^{(j)}$ and $\{\phi_i^{(j)}\}$ are the ith eigenvalue and eigenvector of the jth substructure, respectively. Equation (2) yields n_j eigenvalues: $\Lambda^{(j)} = \mathrm{Diag}\left[\lambda_1^{(j)}, \lambda_2^{(j)}, \dots, \lambda_{nf}^{(j)}\right]$, and the corresponding eigenvectors: $\Phi^{(j)} = \left[\phi_1^{(j)}, \phi_2^{(j)}, \dots, \phi_{nf}^{(j)}\right]$. With mass normalization, one has:

$$\begin{aligned} &[\Phi_i^{(j)}]^T M^{(j)} \Phi^{(j)} = I_{nj} \\ &[\Phi_i^{(j)}]^T K^{(j)} \Phi^{(j)} = \Lambda^{(j)} \end{aligned} \tag{3}$$

Diagonal assembling of the substructures to the primitive form gives:

$$\begin{aligned} &M^p = \mathrm{Diag}[M^{(1)}, M^{(2)}, \dots, M^{(\mathrm{NS})}], K^p = \mathrm{Diag}[K^{(1)}, K^{(2)}, \dots, K^{(\mathrm{NS})}] \\ &\Phi^p = \mathrm{Diag}[\Phi^{(1)}, \Phi^{(2)}, \dots, \Phi^{(\mathrm{NS})}], \Lambda^p = \mathrm{Diag}[\Lambda^{(1)}, \Lambda^{(2)}, \dots, \Lambda^{(\mathrm{NS})}], \end{aligned} \tag{4}$$

where superscript $'p'$ denotes the variables associated with the primitive form, and the size of the above matrices is $\mathrm{NP} \times \mathrm{NP}$. Due to the orthogonality conditions in Eq. (3), it follows that:

$$\begin{aligned} &[\Phi^p]^{\mathrm{T}} M^p \Phi^p = I_{\mathrm{NP}} \\ &[\Phi^p]^{\mathrm{T}} K^p \Phi^p = \Lambda^P. \end{aligned} \tag{5}$$

Reconnection of the primitive system can be performed by considering the geometric compatibility and force equilibrium at the tearing points of the adjacent substructures. If $\{x\}$ is the displacement vector of the original global structure with the size of $N \times 1$, it can be expanded to $\{\bar{x}\}$ with the size of $\mathrm{NP} \times 1$ after substructuring, which includes identical displacements in the tearing DOFs. The geometric compatibility is enforced by applying displacement constraints as:

$$C\{\bar{x}\} = 0, \tag{6}$$

where C is a rectangular matrix containing general implicit constraints to make sure that the nodes at the interface have identical displacement, which is described in Ref. [20]. With the virtual work theorem, the motion equation of the undamped structure is:

$$M^p\{\ddot{\bar{x}}\} + K^p\{\bar{x}\} = F_{\mathrm{ext}} + F_{\mathrm{con}}. \tag{7}$$

For a free vibration system, external excitation force $F_{\mathrm{ext}} = 0$, and the virtual work done by the connection forces F_{con} along $\{\bar{x}\}$ is:

$$\delta W = F_{\mathrm{con}}^{\mathrm{T}}\{\delta \bar{x}\}. \tag{8}$$

Considering the connection process to be incomplete, the compatibility is violated at the tearing coordinates by an amount of $\{\eta\}$. Equation (6) becomes:

$$C\{\bar{x}\} = \{\eta\}. \tag{9}$$

In the new coordinates there will be an associated force vector $\{\tau\}$, representing the internal connection forces due to the 'misfit'. Combination of Eqs. (8) and (9) gives:

$$\delta W = \{\tau\}^{\mathrm{T}}\{\delta\eta\} = \{\tau\}^{\mathrm{T}} C\{\delta\bar{x}\}. \tag{10}$$

From Eqs. (8) and (10), one can obtain:

$$F_{\mathrm{con}}^{\mathrm{T}}\{\delta\bar{x}\} = \{\tau\}^{\mathrm{T}} C\{\delta\bar{x}\}. \tag{11}$$

It is obvious that:

$$F_{\mathrm{con}}^{\mathrm{T}} = C\{\tau\} \tag{12}$$

Consequently, Eq. (7) can be transformed into:

$$\begin{bmatrix} M^p & 0 \\ 0 & 0 \end{bmatrix} \begin{Bmatrix} \ddot{\bar{x}} \\ \ddot{\tau} \end{Bmatrix} + \begin{bmatrix} K^p & -C^{\mathrm{T}} \\ -C & 0 \end{bmatrix} \begin{Bmatrix} \bar{x} \\ \tau \end{Bmatrix} = \begin{Bmatrix} 0 \\ 0 \end{Bmatrix}. \tag{13}$$

Assuming the oscillatory solution of the form $\{\bar{x}, \tau\}^{\mathrm{T}} = \{\bar{\phi}, \tau\}^{\mathrm{T}} \exp\left(i\sqrt{\bar{\lambda}\tau}\right)$, the expanded mode shape of the global structure can be related to the primitive form of the mode shapes Φ^P via the modal coordinates z as [40]:

$$\begin{Bmatrix} \bar{\phi} \\ \tau \end{Bmatrix} = \begin{bmatrix} \Phi^P & 0 \\ 0 & I \end{bmatrix} \begin{Bmatrix} z \\ \tau \end{Bmatrix}, \tag{14}$$

where $\bar{\phi}$ is the expanded mode shape of the global structure including identical values in the interface DOFs. Considering the orthogonality relations in Eqs. (5) and (13) can be transformed into the canonical form:

$$\begin{bmatrix} \Lambda^p - \bar{\lambda} I & -\Gamma \\ -\Gamma^{\mathrm{T}} & 0 \end{bmatrix} \begin{Bmatrix} z \\ \tau \end{Bmatrix} = \begin{Bmatrix} 0 \\ 0 \end{Bmatrix}, \tag{15}$$

where $\Gamma = (C\Phi^p)^{\mathrm{T}}$ is referred to as the normal connection matrix. With the above-described procedure, the nodes at the tearing points of the adjacent structures are constrained to move jointly. Therefore, the eigenvalue $\bar{\lambda}$ obtained with Eq. (15) is equal to the eigenvalue λ belonging to the original global structure. If $\bar{\Phi}$ consists of the expanded eigenvectors $\bar{\phi}$, the eigenvectors of the global structure Φ can be obtained after discarding the identical DOFs in $\bar{\Phi}$. Γ has an order of $\mathrm{NP} \times (\mathrm{NP} - N)$, where $(\mathrm{NP} - N)$ is the number of constraint relations and much less than NP.

The first equation of Eq. (15) gives:

$$z = (\Lambda^p - \bar{\lambda} I)^{-1}\Gamma\tau. \tag{16}$$

Substituting Eq. (16) into the second equation of Eq. (15) to eliminate the modal coordinates z, we have:

$$\Gamma^{\mathrm{T}}(\Lambda^p - \bar{\lambda} I)^{-1}\Gamma\tau = 0 \text{ or } R\tau = 0 \tag{17}$$

in which $R = \Gamma^{\mathrm{T}} D\Gamma$ and $D = (\Lambda^p - \bar{\lambda} I)^{-1}$. The matrix R with the size of $(\mathrm{NP} - N) \times (\mathrm{NP} - N)$, is known as the Kron matrix or receptance matrix [41]. Since the above analysis has no approximation in the derivation of R, the eigenvalues obtained will be identical to the initial structural idealizations which are made in the finite element (FE) modeling of the global structure. $\bar{\lambda}$ is obtained by scanning R's determinant in the original Kron's method [42].

3 Damage detection indices

3.1 Multiple damage location assurance criterion (MDLAC)

Structural damage detection techniques are generally classified into two main categories. They include the dynamic and static identification methods requiring the dynamic and static test data, respectively. Furthermore, the dynamic identification methods have shown their advantages in comparison with the static ones. Among the dynamic data, the modal analysis information of a structure such as the natural frequencies and mode shapes were widely used for damage detection [43]. Determining the level of correlation between the measured and predicted natural frequencies or mode shapes can provide a simple tool for identifying the location and severity of structural damages. When the natural frequencies are employed to identify the damage, two parameter vectors may be determined. A parameter vector consists of the ratios of the first n_{f} natural frequency changes ΔF due to structural damage, that is:

$$\Delta F = \frac{F_{\mathrm{h}} - F_{\mathrm{d}}}{F_{\mathrm{h}}}, \tag{18}$$

where F_{h} and F_{d} denote the natural frequency vectors of the healthy and damaged structure, respectively. Another parameter vector can be similarly defined as:

$$\delta F(X) = \frac{F_{\mathrm{h}} - F(X)}{F_{\mathrm{h}}}, \tag{19}$$

where $F(X)$ is a natural frequency vector that can be predicted from an analytic model and $X^{\mathrm{T}} = \left[x_1, \ldots, x_i, \ldots, x_n\right]$ represents a damage variable vector containing the damage severity $(x_i, i = 1, \ldots, n)$ of all n structural elements.

Given a pair of parameter vectors, one can estimate the level of correlation in several ways. An efficient way is to evaluate a correlation index called the multiple damage location assurance criterion (MDLAC) which is expressed in the following form [43]:

$$\mathrm{MDLAC}(X) = \frac{\left|\Delta F^{\mathrm{T}} \delta F(X)\right|^2}{(\Delta F^{\mathrm{T}} \Delta F)(\delta F^{\mathrm{T}}(X)\delta F(X))}. \tag{20}$$

The MDLAC compares two frequency change vectors, one which is obtained from the examined structure and the other from an analytical model of the structure. The MDLAC varies from a minimum value 0 to a maximum value 1. It will be maximal when the vector of analytical frequencies equals to the frequency vector of the damaged structure, i.e., $F(X) = F_{\mathrm{d}}$.

In many studies, instead of utilizing the natural frequencies for structural damage identification, the mode shape vectors was employed [44]. In this case, the correlation index of Eq. (20) can be expressed as:

$$\mathrm{MDLAC}(X) = \frac{\left|\Delta\varphi^{\mathrm{T}}\delta\varphi(X)\right|^{2}}{(\Delta\varphi^{\mathrm{T}}\Delta\varphi)(\delta\varphi^{\mathrm{T}}(X)\delta\varphi(X))}, \tag{21}$$

where $\Delta\varphi$ is the vector of measured mode shape changes having a dimension equal to the product of the number of measured modes and sensor locations; and $\delta\varphi$ is the vector of analytical mode shape changes with the same dimension of $\Delta\varphi$.

As the both of the indicators given by Eqs. (20) and (21) contain a global characteristic of the structure; therefore, the damage may be located slowly and inaccurately. Accordingly, in this study, an efficient indicator based on the modal strain energy of structural elements containing a local characteristic of the structure is used to locate the damage very quickly and accurately.

3.2 Modal strain energy based index (MSEBI)

In this study, an efficient index based on the modal strain energy (MSE) is used to accurately site the flawed elements of a damaged structure. The modal analysis is a tool to determine the natural frequencies and mode shapes of a structure. It has the mathematical form of [45]:

$$(K - \omega_i^2 M)\varphi_i = 0; \quad i = 1, \ldots, ndf \tag{22}$$

where K and M are the stiffness and mass matrices of the structure, respectively; ω_i and φ_i are the ith circular frequency and mode shape vector of the structure, respectively, and ndf is the total degree of freedom of the structure. The mode shapes are usually normalized with respect to the mass matrix and therefore the relations $\varphi_i^{\mathrm{T}} M \varphi_i = 1$ and $\varphi_i^{\mathrm{T}} K \varphi = \omega_i^2$ can be established.

Since the mode shape vectors are equivalent to nodal displacements of a vibrating structure, therefore, in each element of the structure has the strain energy been stored. The strain energy of a structure due to mode shape vector is usually referred to as modal strain energy (MSE) and can be considered as a valuable parameter for damage identification. The modal strain energy of eth element in ith mode of the structure can be expressed as:

$$\mathrm{mse}_i^e = \frac{1}{2}\varphi_i^{e\mathrm{T}} K^e \varphi_i^e, \quad i = 1, \ldots, ndf,\ e = 1, \ldots, nte, \tag{23}$$

where K^e is the stiffness matrix of eth element of the structure and $\varphi_i^e$is the vector of corresponding nodal displacements of element e in ith mode. The total modal strain energy of ith mode of the structure can also be determined by summation of MSE of all elements nte, which is given by:

$$\mathrm{mse}_i = \sum_{e=1}^{nte} \mathrm{mse}_i^e, \quad i = 1, \ldots, ndf. \tag{24}$$

For the computational purpose, it is better to normalize the MSE of elements with respect to the total MSE of the structure:

$$\mathrm{nmse}_i^e = \frac{\mathrm{mse}_i^e}{\mathrm{mse}_i}, \tag{25}$$

where nmse is the normalized MSE of eth element in ith mode of the structure. The mean of Eq. (25) for the first nm modes can be selected as an efficient parameter as:

$$\mathrm{mnmse}^e = \frac{\sum_{i=1}^{\mathrm{nm}} \mathrm{nmse}_i^e}{\mathrm{nm}}; \quad e = 1, \ldots, nte. \tag{26}$$

In general, when damage occurs in a structural element, it can be simulated by decreasing one of the stiffness parameters of the element such as the elasticity modulus (E) cross-sectional area (A), moment of inertia (I) and so on. Therefore, the damage occurrence is led to increase the MSE and consequently the efficient parameter $\mathrm{mnmse}^e i$. As a result, in this study, by determining the efficient parameter mnmse^e for each element of healthy and damaged structures denoted here as $(\mathrm{mnmse}^e)^{\mathrm{h}}$ and $(\mathrm{mnmse}^e)^{\mathrm{d}}$, respectively, an efficient indicator for estimating the presence and severity of the damage in the element can be defined. This indicator is termed as modal strain energy based index (MSEBI) and can be determined as [46]:

$$\mathrm{MSEBI}^e = \max\left[0, \frac{(\mathrm{mnmse}^e)^{\mathrm{d}} - (\mathrm{mnmse}^e)^{\mathrm{h}}}{(\mathrm{mnmse}^e)^{\mathrm{h}}}\right]; \quad e = 1, \ldots, nte. \tag{27}$$

It should be noted that, as the damage locations are unknown for the damaged structure with respect to real data applications, therefore, for this case the element stiffness matrix of the healthy structure is used for estimating the parameter $(\mathrm{mnmse}^e)^{\mathrm{h}}$. According to Eq. (27), for a healthy element the index will be equal to zero ($\mathrm{MSEBI}^e = 0$) and for a damaged element the index will be larger than zero ($\mathrm{MSEBI}^e > 0$).

4 Bat optimization algorithm

In this study, a bat algorithm (BA) is employed to estimate the damage severity located properly by the MDLAC. The aim is to find a set of reduced damage variables X_r maximizing the MDLACas [30]:

$$\begin{aligned}&\text{Find} \quad X_r^T = \left[x_{r1}, x_{r2}, \dots, x_{rm}\right]\\&\text{Minimize}: \quad \text{OF}(X_r) = 1 - \text{MDLAC}\left(X_r\right)\\&x_{ri} \in R^d, \quad i = 1, \dots, m\end{aligned} \tag{28}$$

where R^d is a given set of discrete values and the damage severity $x_{ri}(i = 1, \dots, m)$ can take values only from this set. OF is an objective function that should be minimized.

BA is a meta-heuristic population-based optimization algorithm which was first inspired from the search of bats to find their food [47]. Bats send some signals to the environment and then listen to their echo which is called echolocation process. BA is mainly constructed by the use of four main ideas [48]: (1) the difference between the prey and food is distinguished through the use of echolocation process; (2) each bat in the position X_i flies with the velocity of V_i producing a special pulse with the frequency and loudness of f_i and A_i respectively; (3) the loudness of A_i changes in different ways such as reducing from a large value to a low value; and (4) the frequency f_i and rate r_i of each pulse is regulated automatically. Initially, all bats fly randomly in the search space producing random pulses. After each fly, the position of each bat is updated as follows:

$$\begin{aligned}&V_i^{\text{new}} = V_i^{\text{old}} + f_i(\text{Gbest} - X_i); \quad i = 1, \dots, N_{\text{Bat}}\\&X_i^{\text{new}} = X_i^{\text{old}} + V_i^{\text{new}}; \quad i = 1, \dots, N_{\text{Bat}}\\&f_i = f_i^{\text{min}} + \varphi_1(f_i^{\max} - f_i^{\min}); \quad i = 1, \dots, N_{\text{Bat}},\end{aligned} \tag{29}$$

where Gbest is the best bat from the objective function point of view; N_{Bat} is the number of bats in the population; $f_i^{\max}/f_i^{\min}$ are the maximum/minimum frequency values of the ith bat and φ_1 is a random value in the range [0, 1]. To reach a better random walking, another random fly is also simulated. In this regard, a random number β is generated randomly. In each iteration, if the random value β is larger than r_1, then a new solution around X_i is generated as follows:

$$X_i^{\text{new}} = X_i^{\text{old}} + \varepsilon A_{\text{mean}}^{\text{old}}; \quad i = 1, \dots, N_{\text{Bat}}, \tag{30}$$

where ε is a random value in the range of [–1, 1] and $A_{\text{mean}}^{\text{old}}$ is the mean value of the loudness of all bats. If the random value β is less than r_1 then a new position X_i^{new} is generated randomly. The new position is accepted if the bellow equation is satisfied:

$$[\beta < A_i] \,\&\, [f(X_i) < f(\text{Gbest})] \tag{31}$$

Also, the values of loudness and rate are updated as follows:

$$\begin{aligned}&A_i^{\text{new}} = \alpha A_i^{\text{old}}\\&r_i^{\text{Iter}+1} = r_i^0[1 - \exp(-\gamma \times \text{Iter})],\end{aligned} \tag{32}$$

where α and γ are constant values and Iter is the number of the iteration during the optimization process.

BA is a powerful algorithm in exploitation (i.e., local search), but at times it may trap into some local optima, so that it cannot perform global search well [49]. For bat algorithm, the search depends completely on random walks, so a fast convergence cannot be guaranteed, therefore, to increase the diversity of the population for BA so as to avoid trapping into local optima, a main improvement of adding passive congregation operator is made to the BA with the aim of speeding up convergence, thus making the approach more feasible for a wider range of practical applications while preserving the attractive characteristics of the basic BA.

5 Bat algorithm optimizer with passive congregation

The update of the velocities and positions of bats is similar to the procedure in the standard PSO [50], as f controls the pace and range of the movement of the swarming particles in essence. To some degree, BA can be considered as a balanced combination of the standard PSO and the intensive local search is controlled by the loudness and pulse rate.

The PSO algorithm is inspired by social behaviors such as spatial order, more especially, aggregation such as bird flocking, fish schooling, or swarming of insects. Each of these cases has stable spatio-temporal integrities of the group of organisms: the group moves persistently as a whole without losing the shape and density [51].

Passive congregation is an attraction of an individual to other group members but where there is no display of social behavior. Social congregations usually happen in a group where the members are related (sometimes highly related). A variety of inter-individual behaviors are displayed in social congregations, necessitating active information transfer [52].

Therefore, each individual in an aggregation has a multitude of potential information from other group members that may minimize the chance of missed detection and incorrect interpretations [52].

Such information transfer can be employed in the model of passive congregation. In original formula of updating of velocity in BA, there is no information sharing among individuals except that Gbest broadcasts the information to the other individuals. Therefore, the population may lose diversity and is more likely to confine the search around local minima if committed too early in the search to the global best found so far. He et al. [51] used passive congregation to proposed the particle swarm optimizer with passive congregation (PSOPC). Inspired by their methods, and to keep the model simple and uniform with BA, we propose a hybrid BA with passive congregation:

$$V_i^{\text{new}} = V_i^{\text{old}} + f_i(\text{Gbest} - X_i) + c_1 r_1 (R_i - X_i),$$

where R_i is a bat selected randomly from the population, c_1 the passive congregation coefficient, and r_1 is a uniform random sequence in the range (0,1): $r_3 \sim U(0, 1)$.

The newly introduced passive congregation coefficient is important for the search performance of EBA. Experiments were executed to select a proper value of c_1. Based on experiments, the best result was generated by EBA with a linearly increasing passive congregation coefficient c_1, which started at 0.4 and ended at 0.6.

6 Main steps for proposed damage detection method

The main steps for the proposed damage detection method using forward substructuring approach, modal strain energy and EBA optimization are summarized as follows:

(a) The global structure is divided into manageable substructures. Each substructure is regarded an independent structure, and the nodes and elements are labeled individually. The stiffness matrices of independent substructures are obtained based on Kron's substructuring method and then, the frequencies and the mode shapes of each substructure are extracted.
(b) Based on Sect. 3.2, MSEBI is used to precisely locate the eventual damages of each substructure.
(c) Setting the number of design variables equal to the number of suspected damaged elements.
(d) Employing EBA to find the optimal solution of Eq. (28) with a few numbers of optimization iterations which leads to obtain the damage severities using MDLAC.

7 Numerical results

In this section, two large-scale space structures are selected as the numerical examples to reveal the robustness and accuracy of the proposed damage detection method. These structures are:

1. A double-layer grid with 200 elements
2. A double-layer barrel vault with 712 elements

In this study, MATLAB [53] is utilized for programming the process while OpenSees [54] is employed for modal analysis. The mass matrix is also assumed to be constant and the structural damages are simulated as a reduction in the Young's modulus of elements in examples. Damage variables are simulated here through a relative reduction of elasticity modulus in each element as:

$$X_i = \frac{E - E_i}{E}, \quad i = 1, \ldots, n, \tag{33}$$

where $E$is the original modulus of elasticity and E_i is the final modulus of elasticity of ith element. The EBA parameters are same for both examples and have been listed in Table 1.

7.1 Example 1: double-layer grid with 200 elements

A double-layer grid with square-on-square pattern, shown in Fig. 1, is considered for damage detection of multiple damage conditions. This space structure has 200 elements, 61 nodes and 171 active degrees of [55]. The material properties of elements include Young's modulus of $E = 2.1 \times 10^2$ GPaand mass density of $\rho = 7850 \frac{\text{kg}}{\text{m}^3}$. The cross-sectional areas of elements in diagonal, bottom and top layers are $A_\text{d} = 10\ \text{cm}^2$, $A_\text{b} = 12\ \text{cm}^2$ and $A_\text{t} = 18\ \text{cm}^2$, respectively.

Table 2 represents two types of damage scenarios with different levels of damage severity. This structure is disassembled into four substructures (NS = 4) with the DOFs of $n1 = 153$, $n2 = 165$, $n3 = 114$, $n4 = 114$, respectively. Figure 2 shows location and boundary of the substructures on global structure. Number of substructures and location of them are estimated by a trial-and-error procedure. However, the proposed method is not sensitive to these choices and can

Table 1 Bat algorithm parameters

Parameter	Description	Value
μ	Population size	50
$f_{\min}$	Minimum frequency	0
$f_{\max}$	Maximum frequency	1
$A_i^0 = A_{\max}$	Initial loudness	1
α	Loudness adaption parameter	0.95
$r_i^0 = r_{\min}$	Initial pulse rate	0.5
γ	Pulse rate adaption parameter	0.98
σ	Standard deviation	2
ρ	Penalty coefficient	1
Niter	Number of iteration	300
c_1	Passive congregation coefficient	Linearly increasing from 0.4 to 0.6

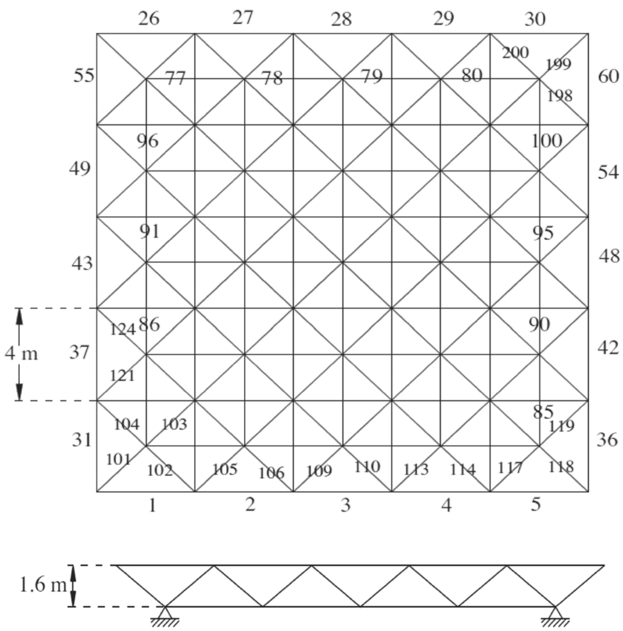

Fig. 1 Double-layer grid with 200 elements

choose any desired number of substructure based on scale of global structure.

It is noticeable that the substructuring methods require dividing the global structure into independent free or fixed substructures. As a free substructure includes the rigid body components, its stiffness matrix is rank deficient and thus cannot be inversed. From the classical eigenequation, the eigenvalues and mass-normalized eigenvectors in modal space are obtained, which include rigid body mode and deformational modes. In this example, the first 20 deformational modes which are selected based on trial-and-error procedure are used for identifying the damage and rigid body modes are neglected.

7.1.1 Locating damages using MSEBI

In the first stage of identifying the induced damages, the modal strain energies of different elements of the double-layer grid for both healthy and damaged structures are determined and then, the indicator MSEBI is evaluated via Eq. (27). Figures 3 and 4 show the value of MSEBI versus element number when global structure is considered and Figs. 5 and 6 show the value of MSEBI for elements of each substructure. It can be observed that in each substructure,

Table 2 Damage scenarios in double-layer grid

Scenario	Damaged element ID in global structure	Substructure ID	Damaged element ID in specified substructure	Damage severity (%)
A	7	1	4	20
	13	3	1	15
	42	1	12	25
	119	2	40	30
	170	3	50	35
B	1	1	1	15
	9	2	5	25
	28	3	10	13
	31	1	7	25
	59	3	23	24
	63	2	18	35
	65	1	15	18
	69	4	18	40
	84	4	25	30
	93	2	26	32
	125	1	39	30
	135	2	48	27
	145	4	34	10
	149	2	54	30
	150	3	38	41
	169	4	48	20
	171	3	51	36
	188	4	57	30
	192	3	64	25

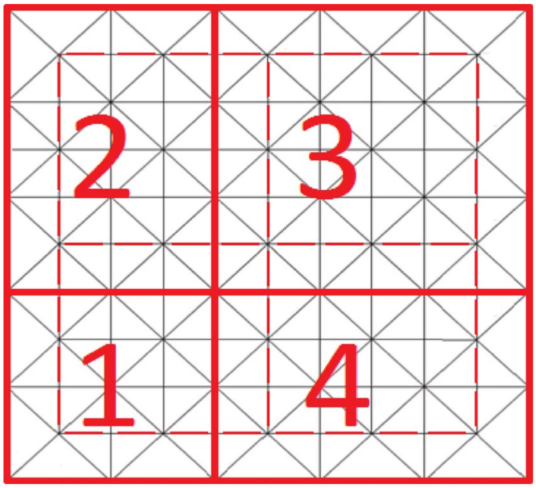

Fig. 2 Substructure's boundary and damaged elements

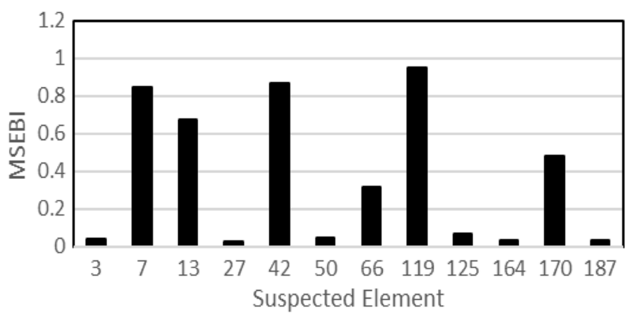

Fig. 3 Suspected damage elements in global structure (scenario A)

MSEBI can accurately locate the damaged elements while in global structure, some of the intact elements are determined as suspected damaged elements. Furthermore, one of the substructures has not any damaged element and it is removed from damage detection process. This is one of advantages of the proposed method, because if substructure is intact, the eigen solution of this part of the structure need not be calculated; while if direct method is used, the eigensolution of global structure should be calculated even if one element is damaged (Figs. 7, 8).

7.1.2 Estimating the damage severity using the EBA

At this stage, the reduced damage detection problem with fewer damage variables instead of 200 original ones can be solved via the optimization algorithm. The EBA is employed to find a set of damage variables maximizing the MDLAC of Eq. (20). The optimization algorithm is applied to solve the problem, and the identified damages, expressed in ratios of elasticity modulus reduction, are shown in Fig. 9. It can be observed that the optimization achieves actual severities of hypothetical damages, while the method presented in Ref. [56] could not accurately identify the damage severities. Based on figures, the overall the root mean square error (RMSE) for damage severity detection using global method is 1.3×10^{-2}; in comparison, the computed error for similar stage in substructure method is 5.12×10^{-3}. The convergence history of EBA can also be seen in Fig. 10 where the MDLAC value versus iteration number during the optimization process is shown. It can be observed that when substructures considered, the optimization converges to actual damage severities mostly after only three iterations. It means that only a few finite element analyses (FEA) are needed during the optimization process. When global structure is considered in second stage, the process of finding optimal solution takes 602 s to reach the best solution while the total time of this process using substructuring is 43 s and it is 7.42% of latter (Fig. 11). Therefore, using substructuring approach, the process of damage detection in large-scale space structures will be faster and more accurate.

Fig. 4 Suspected damage elements in global structure (scenario B)

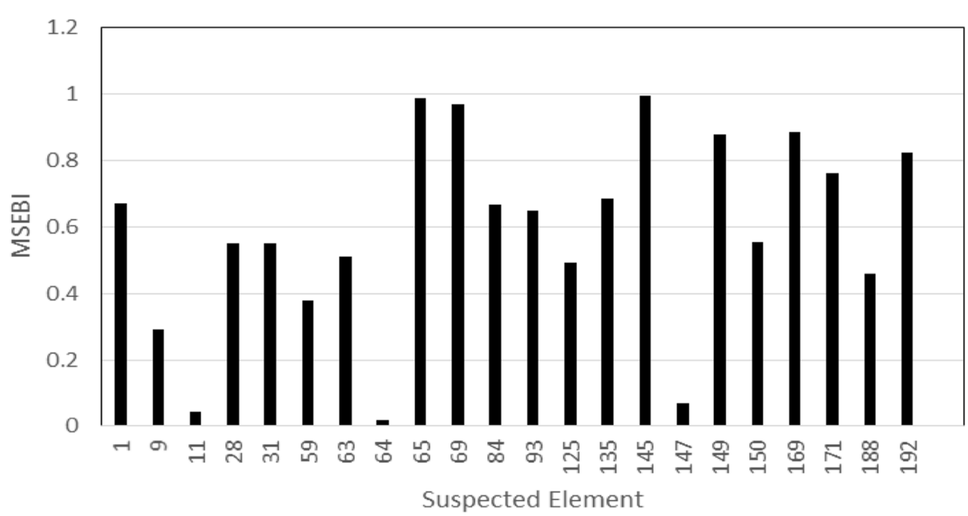

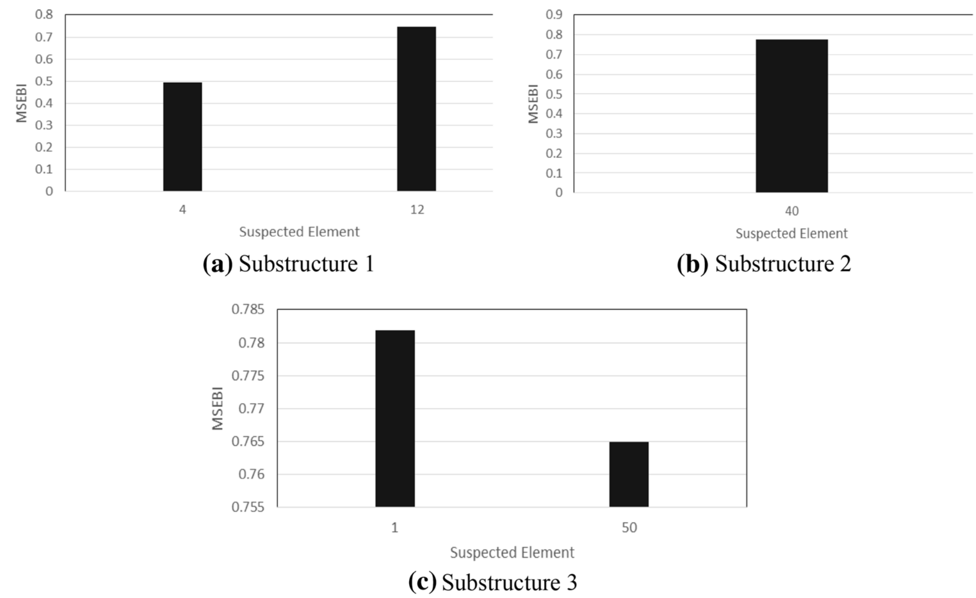

Fig. 5 Suspected damage elements in substructures (scenario A)

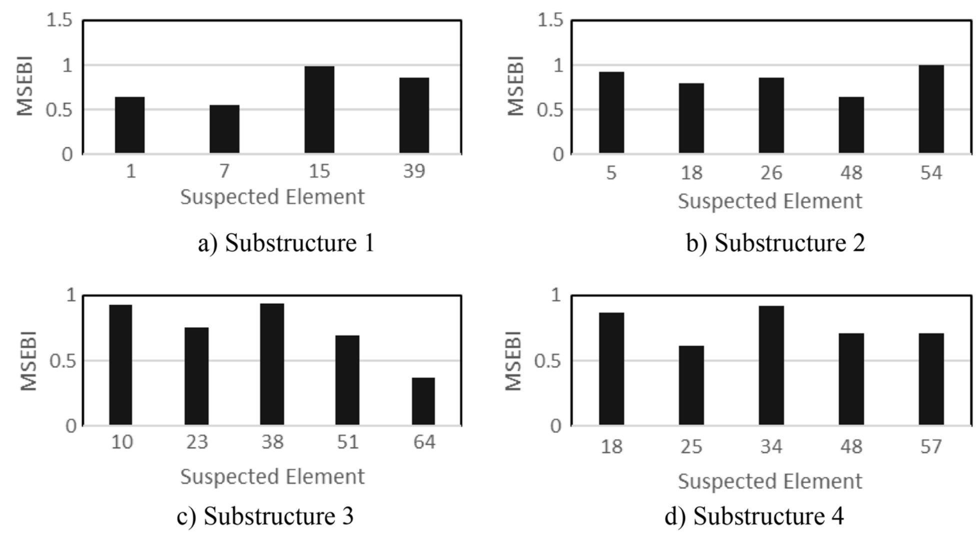

Fig. 6 Suspected damage elements in substructures (scenario B)

7.2 Example 2: double-layer barrel vault

To demonstrate the robustness of the proposed method, a double-layer barrel vault with covering surface 30×40 m is considered, for damage identification of multiple damage conditions [57]. This space structure with 721 elements and 200 nodes is shown in Fig. 12. The cross-sectional areas of elements in diagonal, bottom and top layers are $A_d = 26.75\ \text{cm}^2$, $A_b = 30.34\ \text{cm}^2$ and $A_t = 39.52\ \text{cm}^2$, respectively. The mass density and the Young's modulus are assumed to be $\rho = 7850\ \frac{\text{kg}}{\text{m}^3}$ and $E = 2.1 \times 10^2$ GPa. Two damage scenarios shown in Table 3 are assumed in this example. This structure is disassembled into four substructures same as previous example (NS = 4) with the DOFs of $n1 = 251$, $n2 = 265$, $n3 = 214$, $n4 = 134$, respectively.

7.2.1 Locating the damage using MSEBI

The first stage of the proposed method is performed for each scenario and the results are shown in Figs. 13 and 14 for global structure and Fig. 15 for substructures. However, result of locating suspected damage elements and detecting severity of damage for substructures in scenario B is not given here because of the paper length limitation.

These figures show that when global structure considered, the variables reduce from 721 elements to 7 elements in scenario A and 14 elements in scenario B, but there is an obvious error in the estimating number of damaged elements in these cases. While when we use substructuring method, only real damaged elements are chosen as the suspected damage elements in this stage.

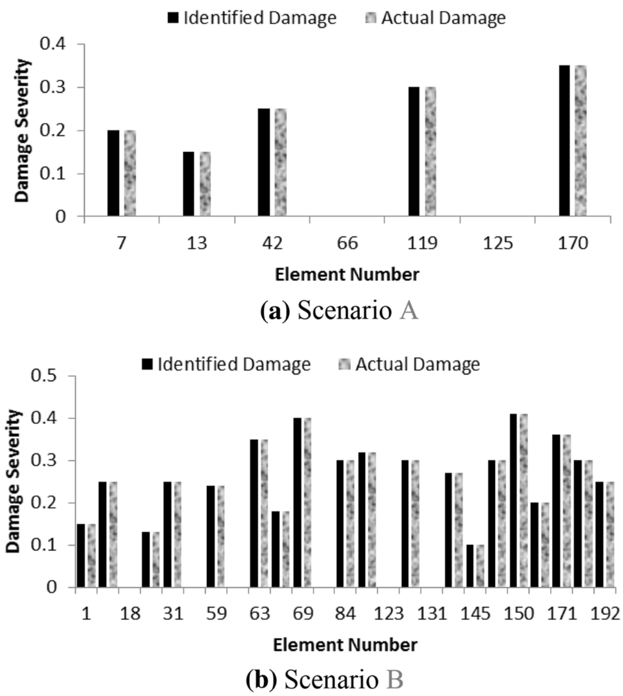

(a) Scenario A

(b) Scenario B

Fig. 7 Damage severities of global structure

This is due to the fact that the local damage has a slight effect on global stiffness matrix and eigenparameters, whereas the substructural eigenparameters are still sensitive to the local damage by concerning the local area as an independent structure. The global eigenparameters caused by the local damage are sometimes smaller than those caused by measurement noise, which makes the damage detection difficult to be conducted based on global eigenparameters directly. The substructural eigenparameters focus on local area and thus bear larger changes caused by local damage.

7.2.2 Estimating the damage severity using the EBA

The results of damage severities estimated in different scenarios are shown in Figs. 16 and 17 using the EBA. These figures show that some of the intact elements are removed in the third stage of damage detection, though they are chosen as the suspected damage elements in the second stage. Furthermore, when global structure is considered in second stage, the process of finding optimal solution takes 781 s to reach the best solution, while the total time of this process for substructure is 32 s and it is 4.2% of latter.

Figure 16 represents that when global structure is considered, the accuracy of damage severity detection can decrease for the case in which a lot of damaged elements exist and in some cases, intact element is chosen as a damaged element. While using substructuring method, this obvious error is removed. Furthermore, based on figures, the overall the root mean square error (RMSE) for damage severity detection using global method is 1.9×10^{-2}; in comparison, computed error for the similar stage in substructure method is 7.49×10^{-3}.

Finally, Fig. 18 shows comparison of computation time of damage severity detection using BA method versus EBA; based on result, our EBA outperformed the original BA algorithms in terms of accuracy and convergence rate.

8 Discussion of results

The three-stage methodology that is proposed in this paper outperformed the other methodologies for damage detection of large-scale space structure. This is due to the third stage of our proposed method, where the analytic model of structure is updated in each iteration until the MDLAC will be maximized, and therefore, the vector of analytical

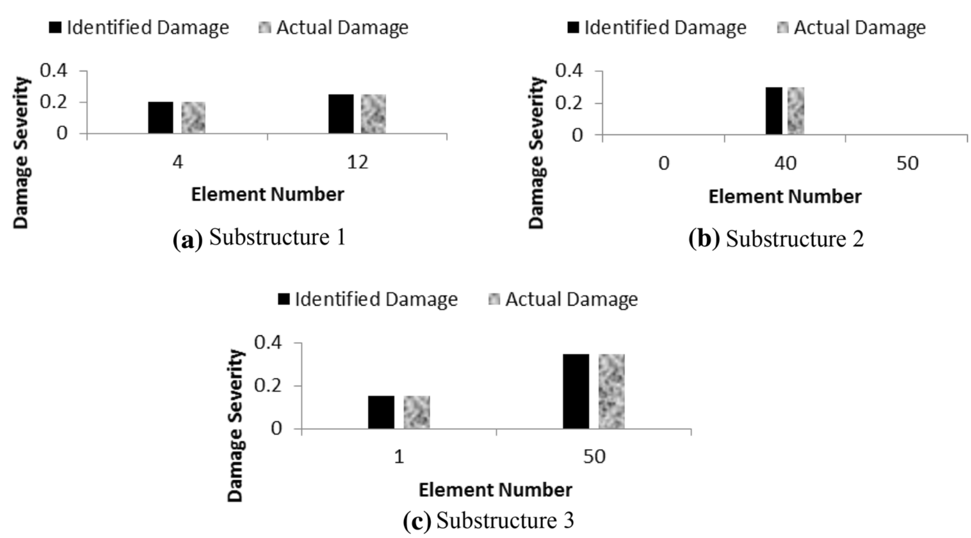

(a) Substructure 1

(b) Substructure 2

(c) Substructure 3

Fig. 8 Damage severities of substructures (scenario A)

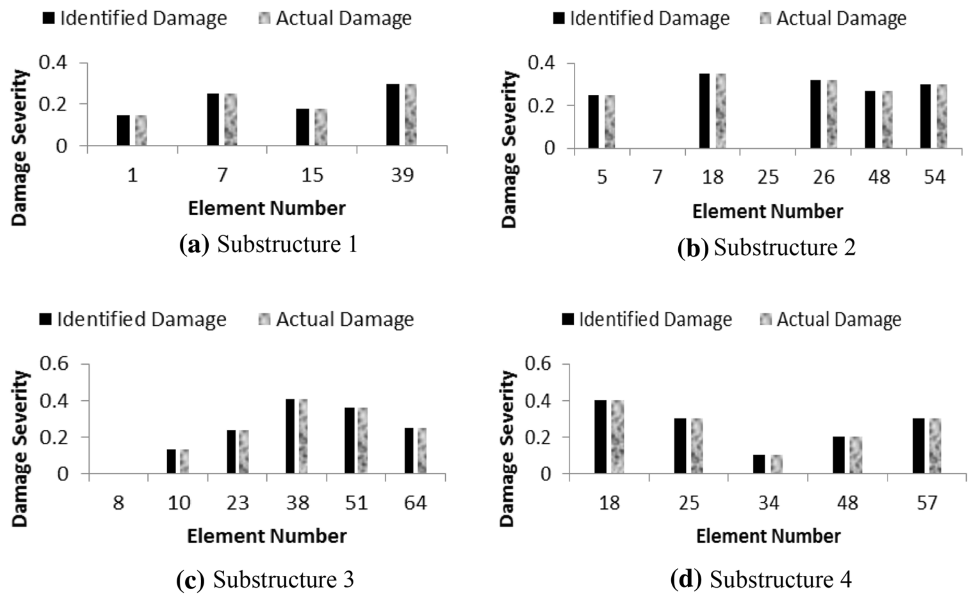

Fig. 9 Damage severities of substructures (scenario B)

frequencies would be equal to the frequency vector of damaged structure. Generally, during FE model updating process, elemental parameters in the FE model are iteratively modified, so that the modal properties (such as frequencies and mode shapes) match the measured counterparts in an optimal way [39]. To achieve this, the eigensolutions of the analytical model need to be calculated repeatedly [2]. When tackling large-scale structures, three major difficulties arise. First, since the analytical model of a large-scale structure consists of many degrees of freedom (DOFs), the resulting mass matrix and stiffness matrix need very large space to store. Second, and more importantly, the computation effort may be great in extracting the eigensolutions from the mass and stiffness matrices, which need to be calculated repeatedly. Third, the number of parameters that need to be updated in a large-scale structure can be large, which may hinder the convergence of the optimization process. To overcome these difficulties, the substructuring method is a good preference. First, it is possible to analyze each substructure independently, or even concurrently with parallel computing [58]. While identical substructures exist, the computation load is reduced further. Second, when only particular substructures need to be focused on, it is more efficient to calculate the eigensolutions of the particular substructures iteratively during the model updating process. Third, the number of parameters updated in each substructure is much less than that in the global structure. This improves the convergence rate of model updating process. Handling smaller problems at a time can improve the accuracy of the solutions since accumulated error during the computation is reduced.

In addition, MSEBI damage index is used in the second stage to properly locate eventual damage elements; this stage reduces damage variables and accelerates the performance of the third stage to accurately estimate the damage extent using EBA.

Finally, EBA outperformed the original BA algorithms because the passive congregation operator can be regarded as a stochastic variable that introduces perturbations to the search process [59]. For each individual, the turbulence (perturbation) is proportional to the distance between itself and a randomly selected neighborhood rather than an external random number. In the early search process, the distances between individuals are large, therefore, the turbulence is large, which may allow the swarm to avoid converging to a poor local minimum. As the generations increase, the distances between individuals become smaller, therefore, the turbulence becomes smaller, which enables the swarm to refine solutions.

9 Conclusion

In this study, a three-stage damage detection method is proposed for the large-scale space structures. First, global structure is divided into manageable substructures. The stiffness matrices of independent substructures are obtained based on Kron's substructuring method. The substructural stiffness matrix and its eigenparameters are used as the indicators for the damage detection. The substructuring method concerns the local area by treating it as an independent structure. The substructural stiffness and eigenparameters are more sensitive to the damage, and thus they are better to be used in the damage detection domain. The suspected damage locations are detected by comparing the variations in modal strain energy of the intact and the damaged structures. Afterward, the damage severities are estimated by employing the

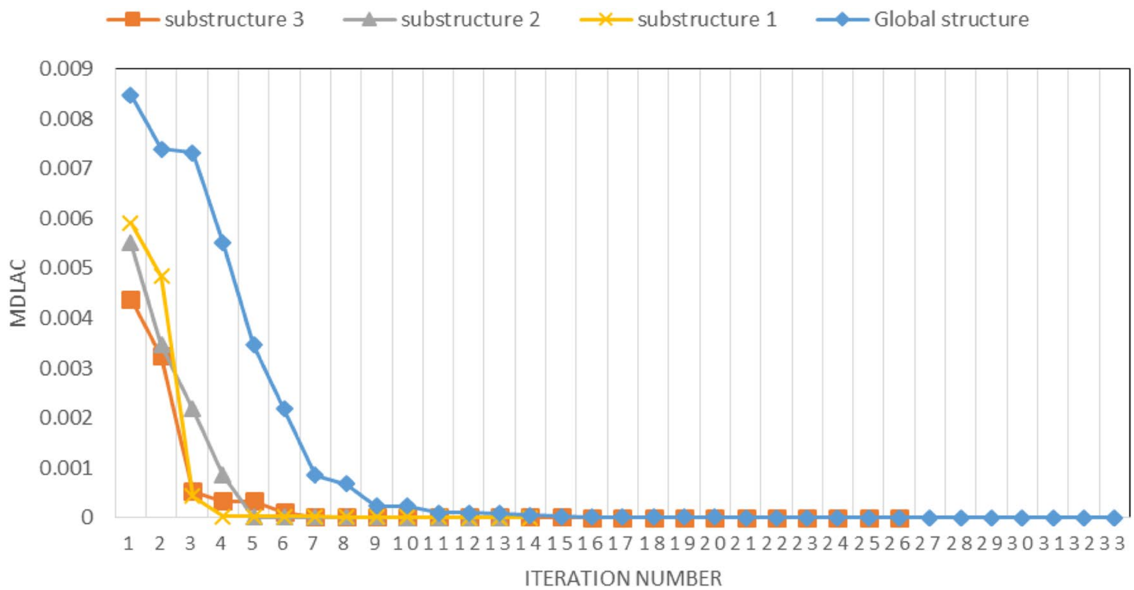

(a) Scenario A

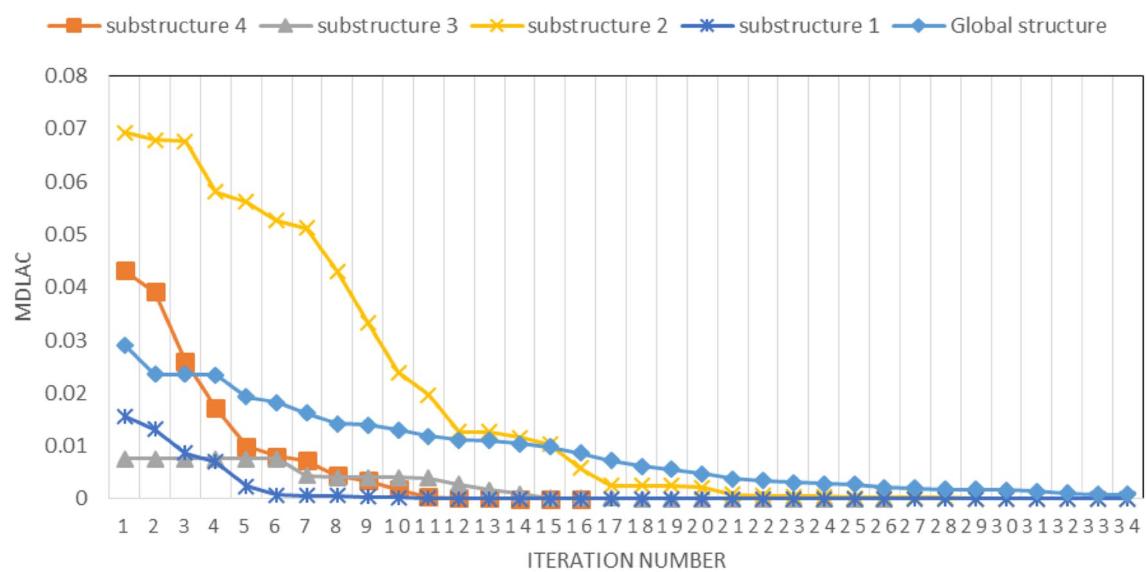

(b) Scenario B

Fig. 10 Convergence history of EBA

MDLAC and an iterative optimization algorithm such as EBA.

The effectiveness of the proposed substructuring method for damage detection is verified through the application to large-scale space structures. The results are compared with the case in which the global structure is considered. The results illustrated the high performance and accuracy of the proposed method for the damage detection of large-scale space structures with multiple damages. Employing modal strain energy of the structural elements in the first stage of damage detection largely reduces the number of variables from the total elements to a number of suspected damaged elements. Moreover, using MDLAC values and EBA algorithm in the third stage of the damage detection is more efficient for estimating the damage severities.

Furthermore, compared with the global eigenparameters, the substructural eigenparameters have larger changes due to the local damages, and thus are more sensitive to the local damages. The local damages have a slight effect on the global stiffness matrix and eigen parameters; however, the substructural eigenparameters are still sensitive to the local damages by concerning the local area as an independent

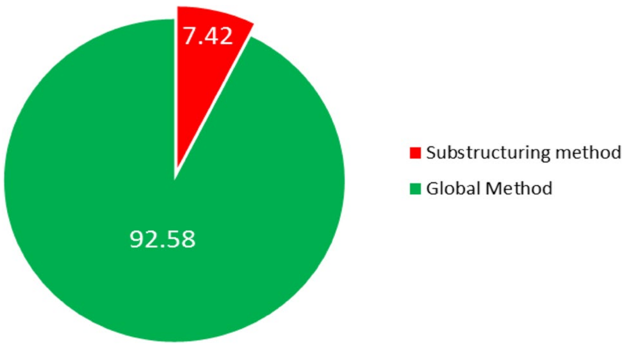

Fig. 11 Comparison of computation time of damage severity detection using substructuring method versus global method

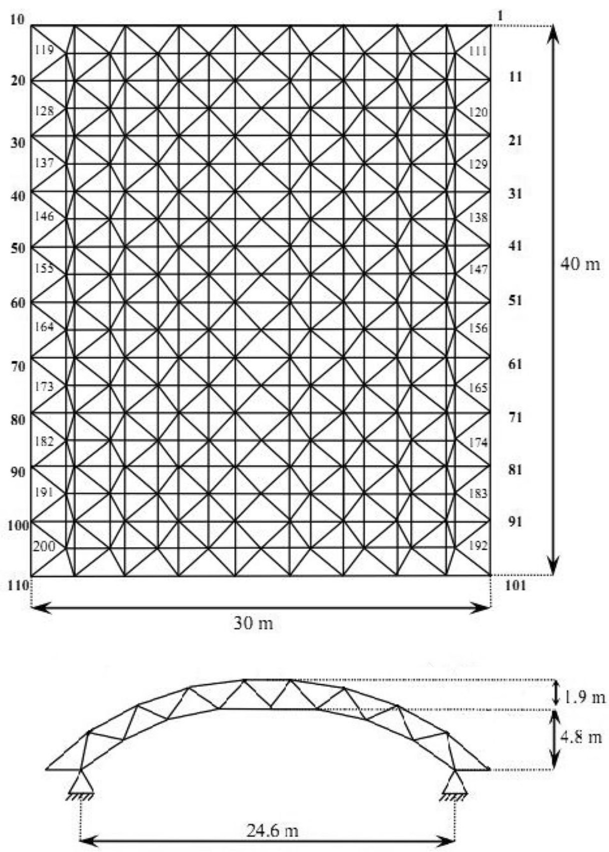

Fig. 12 Double-layer barrel vault

structure. Hence, the substructural eigenparameters are preferable to be used for damage detection and related applications of structural health monitoring.

In addition, the process of damage detection in large-scale space structures will be faster and more accurate using substructuring approach. The computational time of the damage severity detection using EBA engaged by the substructuring method is significantly reduced in comparison with the use of the direct FE model of global structure based on EBA (about one-tenth) which is further highlighted in the damage detection of the large-scale structures.

Finally, the results represent that the proposed method can detect the locations and severity of the damages in all damage cases such as small and large damage severities and also multiple damage cases. Therefore, the proposed method is very efficient for the damage detection of the large-scale space structures with a great number of elements and can be used in practical situations.

Finally, in this paper, a new BA with the passive congregation (EBA) has been presented based on the standard BA. By introducing passive congregation, information can be transferred among individuals that will help individuals to avoid misjudging information and being trapped by poor local minima. The only coefficient introduced into the standard BA is the passive congregation coefficient c. A generic value of c was selected by experiments. The results indicated that with the considered examples, EBA performed significantly better than standard BA.

Table 3 Damage scenarios in double-layer barrel vault

Scenario	Damaged element ID in global structure	Substructure ID	Damaged element ID in specified substructure	Damaged severity (%)
A	175	1	36	10
	248	4	17	20
	542	4	98	30
	701	1	65	60
B	17	2	12	15
	187	1	51	20
	201	3	10	30
	354	4	72	60
	472	2	103	70
	555	4	118	80
	672	1	63	90

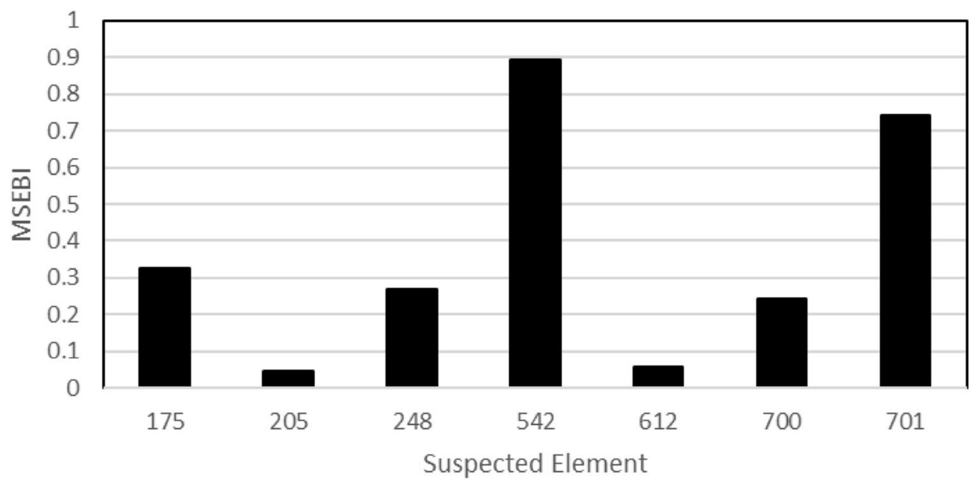

Fig. 13 Suspected damage elements in global structure (scenario A)

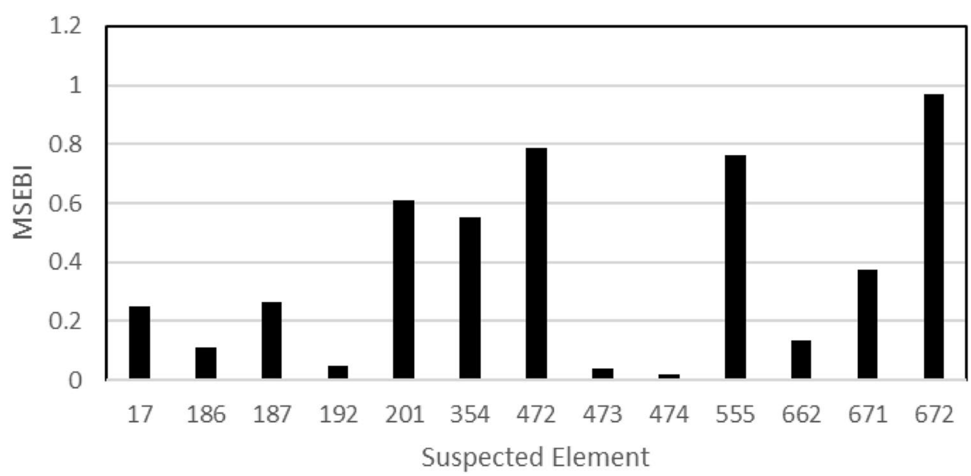

Fig. 14 Suspected damage elements in global structure (scenario B)

Fig. 15 Suspected damage elements in substructures (scenario B)

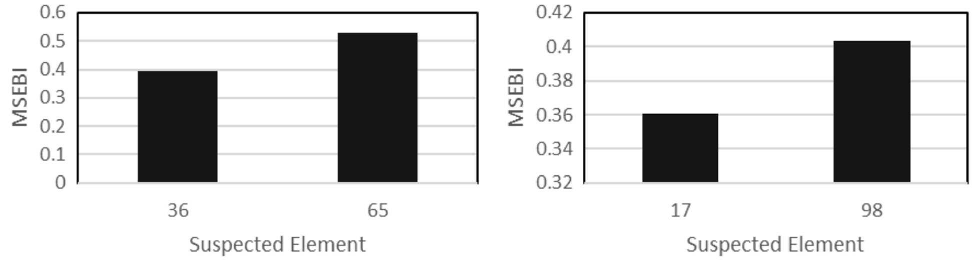

(a) Substructure 1 **(b)** Substructure 4

Fig. 16 Damage severity of global structure

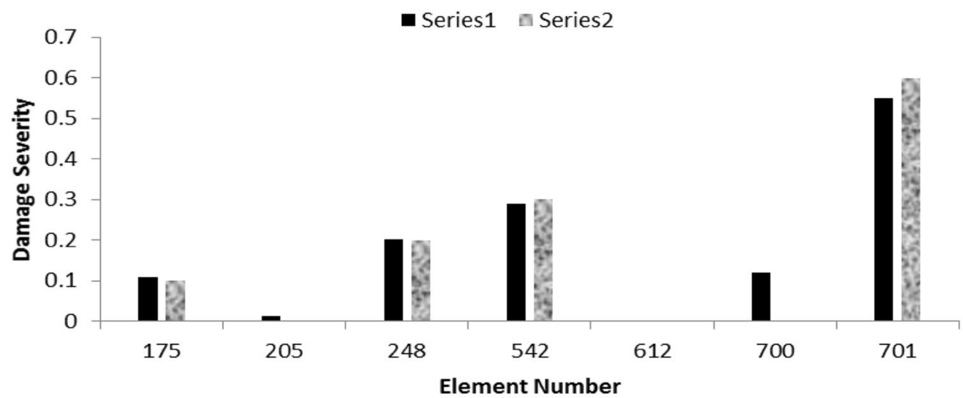

(a) Scenario A

(b) Scenario B

Fig. 17 Damage severity of substructures (scenario B)

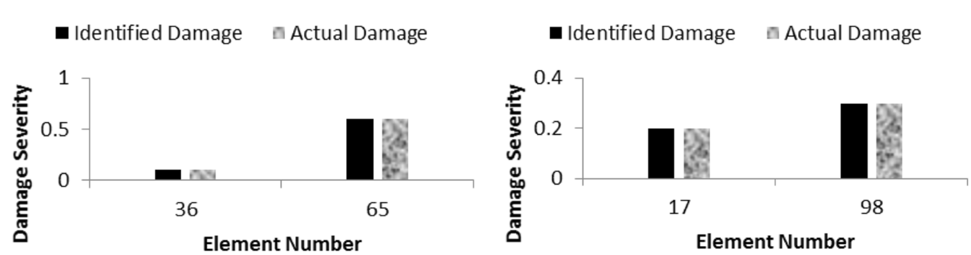

(a) Substructure 1 **(b)** Substructure 4

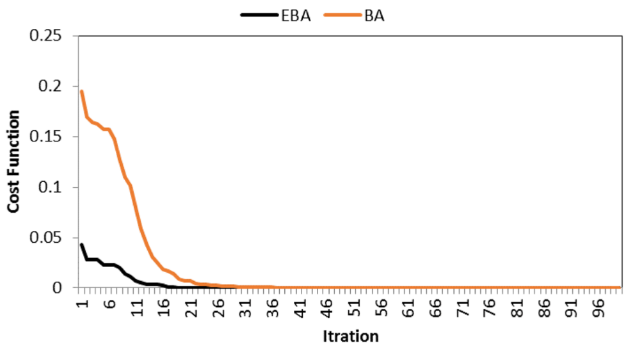

Fig. 18 Comparison of computation time of damage severity detection using BA method versus EBA

References

1. Beygzadeh S, Salajegheh E, Torkzadeh P, Salajegheh J, Naseralavi S (2014) An improved genetic algorithm for optimal sensor placement in space structures damage detection. Int J Space Struct 29:121–136
2. Farrar CR, Worden K (2007) An introduction to structural health monitoring. Philos Trans R Soc A Math Phys Eng Sci 365(1851):303–315
3. Goyal D, Pabla BS (2015) The vibration monitoring methods and signal processing techniques for structural health monitoring: a review. Arch Comput Methods Eng 23(4):585–594. https://doi.org/10.1007/s11831-015-9145-0
4. Fan W, Qiao P (2011) Vibration-based damage identification methods: a review and comparative study. Struct Heal Monit 10(1):83–111
5. Naseralavi SS, Salajegheh J, Salajegheh E, Fadaee MJ (2010) An improved genetic algorithm using sensitivity analysis and micro search for damage detection. Asian J Civ Eng v11 i6:717–740
6. Kim J-B, Lee E-T, Rahmatalla S, Eun H-C (2013) Non-baseline damage detection based on the deviation of displacement mode shape data. J Nondestruct Eval 32(1):14–24
7. Yoon MK, Heider D, Gillespie JW, Ratcliffe CP, Crane RM (2010) Local damage detection with the global fitting method using operating deflection shape data. J Nondestruct Eval 29(1):25–37
8. Guo HY, Li ZL (2011) Two-stage multi-damage detection method based on energy balance equation. J Nondestruct Eval 30(3):186–200
9. Amiri GG, Hosseinzadeh AZ, Razzaghi SAS (2015) Generalized flexibility-based model updating approach via democratic particle swarm optimization algorithm for structural damage. Int J Optim Civ Eng 5:445–464
10. Monajemi H, Razak HA, Ismail Z (2013) Damage detection in frame structures using damage locating vectors. Measurement 46:3541–3548
11. Varmazyar M, Haritos N (2015) A Bayesian damage identification technique using evolutionary algorithms—a comparative study. Electron J Struct Eng 14(1):1–19
12. Alampalli S (1998) Influence of in-service environment on modal parameters. Proc Spie Int Soc Opt Eng 1:111–116
13. Maeck J, De Roeck G (2003) Damage assessment using vibration analysis on the Z24-bridge. Mech Syst Signal Process 17(1):133–142
14. Robert GL, John TD (2006) Ambient vibration monitoring of a highway bridge undergoing a destructive test. J Bridg Eng 11(5):602–610
15. Xia Y, Hao H, Zanardo G, Deeks A (2006) Long term vibration monitoring of an RC slab: temperature and humidity effect. Eng Struct 28(3):441–452
16. Torkzadeh P, Goodarzi Y, Salajegheh E (2013) A two-stage damage detection method for large-scale structures by kinetic and modal strain energies using heuristic particle swarm optimization. Int J Optim Civ Eng 3(3):465–482
17. Craig RR (2000) Coupling of substructures for dynamic analyses: an overview. AIAA Pap 1573:2000
18. Weng S, Xia Y, Xu Y-L, Zhu H-P (2011) Substructure based approach to finite element model updating. Comput Struct 89(9):772–782
19. Weng S, Xia Y, Xu Y-L, Zhu H-P (2011) An iterative substructuring approach to the calculation of eigensolution and eigensensitivity. J Sound Vib 330(14):3368–3380
20. Xia Y, Weng S, Xu Y-L, Zhu H-P (2010) Calculation of eigenvalue and eigenvector derivatives with the improved Kron's substructuring method. Struct Eng Mech 36(1):37–55
21. Ghiasi R, Torkzadeh P, Noori M (2016) A machine-learning approach for structural damage detection using least square support vector machine based on a new combinational kernel function. Struct Heal Monit 15(3):302–316
22. Fathnejat H, Torkzadeh P, Salajegheh E, Ghiasi R (2014) Structural damage detection by model updating method based on cascade feed-forward neural network as an efficient approximation mechanism. Int J Optim Civ Eng 4(4):451–472
23. Ghiasi R, Ghasemi MR, Noori M (2018) Comparative studies of metamodeling and AI-based techniques in damage detection of structures. Adv Eng Softw
24. Gholizadeh S, Seyedpoor SM (2011) Shape optimization of arch dams by metaheuristics and neural networks for frequency constraints. Sci Iran 18(5):1020–1027
25. Gholizadeh S, Shahrezaei AM (2015) Optimal placement of steel plate shear walls for steel frames by bat algorithm. Struct Des Tall Spec Build 24(1):1–18
26. Gholizadeh S, Poorhoseini H (2015) Optimum design of steel frame structures by a modified dolphin echolocation algorithm. Struct Eng Mech 55(3):535–554
27. Lopes S, Gomes GF, Mendez YAD, P da SL Alexandrino, da Cunha SS, Ancelotti AC (2018) A review of vibration based inverse methods for damage detection and identification in mechanical structures using optimization algorithms and ANN. Arch Comput Methods Eng 4(1):1–15
28. Llc CRCP, Liu G-R, Han X (2003) Computational inverse techniques in nondestructive evaluation. CRC Press, Boca Raton
29. Gandomi AH, Yang X-S, Alavi AH, Talatahari S (2013) Bat algorithm for constrained optimization tasks. Neural Comput Appl 22(6):1239–1255
30. Nobahari M, Seyedpoor SM (2013) An efficient method for structural damage localization based on the concepts of flexibility matrix and strain energy of a structure. Struct Eng Mech 46(2):231–244
31. Torkzadeh P, Khamseh M (2014) Structural engineering a two-stage damage detection method for truss structures using FRF data and LMPSO algorithm. Iran J Struct Eng 1(2):114–125
32. Jiang S, Zhang C, Zhang S (2011) Two-stage structural damage detection using fuzzy neural networks and data fusion techniques. Expert Syst Appl 38(1):511–519
33. Catbas N, Malekzadeh M, Gul M, Kwon I-B (2014) An integrated approach for structural health monitoring using an in-house built fiber optic system and non-parametric data analysis. Smart Struct Syst 14(5):917
34. Malekzadeh M, Atia G, Catbas FN (2015) Performance-based structural health monitoring through an innovative hybrid data interpretation framework. J Civ Struct Heal Monit 5(3):287–305

35. Ghiasi R, Torkzadeh P, Noori M (2014) Structural damage detection using artificial neural networks and least square support vector machine with particle swarm harmony search algorithm. Int J Sustain Mater Struct Syst 1(4):303–320
36. Fathnejat H, Ghiasi R, Torkzadeh P (2016) Damage detection of plate-like structures using intelligent surrogate model. Smart Struct Syst 18(6):159–189
37. Matarazzo TJ, Pakzad SN (2016) Truncated physical model for dynamic sensor networks with applications in high-resolution mobile sensing and BIGDATA. J Eng Mech 142(5):1–13
38. Jia F, Lei Y, Lin J, Zhou X, Lu N (2016) Deep neural networks: a promising tool for fault characteristic mining and intelligent diagnosis of rotating machinery with massive data. Mech Syst Signal Process 72:303–315
39. Simpson A (1973) A generalization of Kron's eigenvalue procedure. J Sound Vib 26:129–139
40. Bathe JKJ, Wilson EL (1989) Numerical methods in finite element analysis. Prentice-Hall, Inc., Englewood Cliffs
41. Weng S, Xia Y, Xu Y-L, Zhou X-Q, Zhu H-P (Jun. 2009) Improved substructuring method for eigensolutions of large-scale structures. J Sound Vib 323(3–5):718–736
42. Simpson A (1974) Scanning Kron's determinant. Q J Mech Appl Mech 27:27–43
43. Messina A, Williams EJ, Contursi T (1998) Structural damage detection by a sensitivity and statistical-based method. J Sound Vib 216(5):791–808
44. Guo HY, Li ZL (2009) A two-stage method to identify structural damage sites and extents by using evidence theory and micro-search genetic algorithm. Mech Syst Signal Process 23(3):769–782
45. Paz M (1997) Structural dynamics: theory and computation. Springer, New York
46. Seyedpoor SM (2012) A two stage method for structural damage detection using a modal strain energy based index and particle swarm optimization. Int J Non Linear Mech 47(1):1–8
47. Yang X-S, Gandomi AH (2012) Bat algorithm: a novel approach for global engineering optimization. Eng Comput 29(5):464–483
48. Komarasamy G, Wahi A (2012) An optimized K-means clustering technique using bat algorithm. Eur J Sci Res 84(2):263–273
49. Wang G, Guo L (2013) A novel hybrid bat algorithm with harmony search for global numerical optimization. J Appl Math 2013:1–21
50. Kennedy J (2010) Particle swarm optimization. In: Encyclopedia of machine learning. Springer, New York, pp 760–766
51. He S, Wu QH, Wen JY, Saunders JR, Paton RC (2004) A particle swarm optimizer with passive congregation. Biosystems 78(1):135–147
52. Parrish JK, Hamner WM (1997) Animal groups in three dimensions: how species aggregate. Cambridge University Press, Cambridge
53. Release M (2012) The MathWorks. MathWorks. Inc., Natick
54. McKenna F, Fenves GL, Scott MH, Jeremic B (2000) Open System for earthquake engineering simulation (OpenSees). Pacific Earthquake Engineering Research Center. University of California, Berkeley
55. Gholizadeh S, Salajegheh E, Torkzadeh P (2008) Structural optimization with frequency constraints by genetic algorithm using wavelet radial basis function neural network. J Sound Vib 312(1–2):316–331
56. Koh BH, Dyke SJ (Feb. 2007) Structural health monitoring for flexible bridge structures using correlation and sensitivity of modal data. Comput Struct 85(3–4):117–130
57. Salajegheh E, Gholizadeh S (2005) Optimum design of structures by an improved genetic algorithm using neural networks. Adv Eng Softw 36(11–12):757–767
58. Lallemand B, Level P, Duveau H, Mahieux B (1999) Eigensolutions sensitivity analysis using a sub-structuring method. Comput Struct 71(3):257–265
59. Cai X, Wang L, Kang Q, Wu Q (2014) Bat algorithm with Gaussian walk. Int J Bio-Inspired Comput 6(3):166–174

Publisher's Note Springer Nature remains neutral with regard to jurisdictional claims in published maps and institutional affiliations.